Spatial Noise Reduction by Optical Filters in Mercury Cadmium Telluride Hybrid Focal Plane Arrays

Vishnu Gopal and S.K. Singh
Solidstate Physics Laboratory, Delhi–110 054

ABSTRACT

This paper discusses the role of optical filters in the reduction of spatial noise in Hg_{1-x} Cd_xTe hybrid focal plane arrays (FPAs). It is shown that optical filters of appropriate cut-off wavelength can cause considerable reduction in the spatial noise of both mid-wavelength infrared (MWIR) and long-wavelength infrared (LWIR) arrays. These filters can result in considerable improvement in the NETD performance of a MWIR *HgCdTe* FPA, whereas in LWIR FPAs, these can also be used to trade-off the requirement of composition uniformity of the *HgCdTe* substrate, depending upon the relative magnitude of temporal and spatial noise components.

Keywords: Optical filters, spatial noise, temporal noise, NETD performance, *HgCdTe* FPAs, MWIR arrays, LWIR arrays

1. INTRODUCTION

Minimising spatial noise ($I_{N,\,spatial}$) (pixel-to-pixel response variations) in a staring *HgCdTe* hybrid focal plane array (FPA) has always been the key concern of the scientists and engineers engaged in the development of this device. What matters ultimately in the application is the residual spatial noise, in the FPA after applying a non-uniformity compensation[1-7] algorithm. Often, a two-point linear compensation scheme is used to compensate the response variations. Complex schemes, such as a piecewise linear compensation technique though can lead to smaller residual spatial noise have not found favour due to the associated complexities in the real-time calibration of FPAs. This study shows that an optical filter with appropriate cut-off wavelength can lead to considerable reduction in the residual spatial noise while still using a two-point linear complex algorithm.

2. ROLE OF OPTICAL FILTER

It is well known that cut-off wavelength of the $Hg_{1-x}Cd_xTe$ IR detectors vary with variation in the composition of the base material. The spread in detector cut-off wavelength ($\Delta\lambda_{co}$) with the composition non-uniformity (Δx) within the substrate will be given by:

$$\Delta\lambda_{co} = \lambda_{co}\frac{1}{E_g}\left(\frac{\Delta E_g}{\Delta x}\right)\Delta x \qquad (1)$$

Based on the known dependence of the band gap of $Hg_{1-x}Cd_xTe$ on its composition[8] x, $\Delta E_g/\Delta x$ is

Received 18 October 2000

The plot of Eqn (1) shown in Fig. 1 suggests that the small composition non-uniformities in the base material can lead to considerable spread in the cut-off wavelength of the photodetectors in the array. These variations in the cut-off wavelength lead to the non-uniform response spatial noise of the pixels in the FPA. The residual spatial noise after applying a two-point linear compensation scheme will therefore obviously be a sensitive function of Δx.

One way of reducing the residual spatial noise on account of composition variations is to use substrate of high composition uniformity. Alternatively, optical filters with cut-off wavelength less than the average detector cut-off wavelength can be externally employed to obtain the same effect. These filters limit the wavelength range of incident radiation forcing a more uniform integrated response of the photodiodes to the incident radiation. These are only qualitative considerations and one would like to know quantitatively the effect of the cut-off wavelength

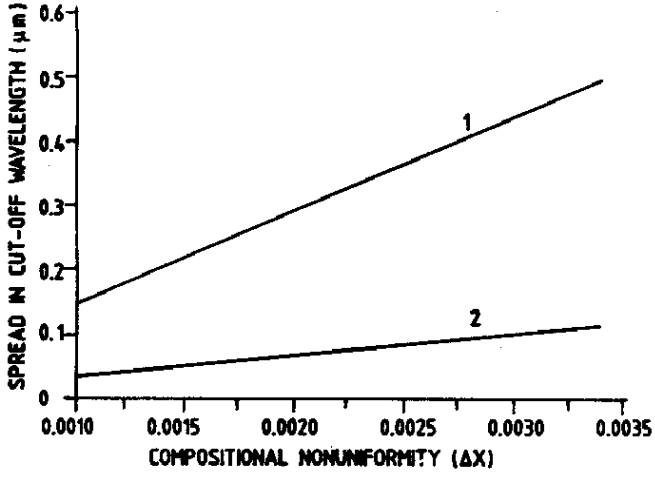

Figure 1. Calculated spread ($\Delta\lambda_{co}$) in the detector cut-off wavelengths in an Hg_{1-x} Cd_xTe FPA *vs* composition non-uniformity (Δx) within the substrate. The respective curves marked 1 and 2 correspond to mean detector cut-off wavelengths 5.1 μm and 10.6 μm.

the integration time (T_i) has also been discussed. The purpose is to present an analytical approach for calculating the performance of *HgCdTe* FPAs as a function of the cut-off wavelength of the optical filter.

3. MODEL

In practice, one of the objectives of using these filters should be to reduce the spatial noise below the level of mean temporal noise ($I_{N,\,temporal}$) without degrading the overall noise equivalent temperature difference (NETD) performance of the FPA due to the loss of signal on account of smaller cut-off wavelength of the optical filter. It was therefore proposed to carry out a study of relative temporal and spatial noise contributions and the corresponding NETDs as a function of the cut-off wavelength of the filter for a given configuration of FPA. FPA consisting of *HgCdTe* photovoltaic detectors source coupled to a silicon read-out multiplexer has been considered. The input to the read-out multiplexer is assumed to be consisting of metal oxide semiconductor field-effect transistor (MOSFET) channel (operating in the weak inversion mode) with a buffered direct injection (BDI) interface circuit.

3.1 Spatial Noise

Assuming a Gaussian distribution of pixel responses in a given FPA, the uncorrected spatial noise can be defined[9], as the observed or estimated deviation from the mean pixel response to the $\pm 1\sigma$ points of the response distribution curve. The corresponding residual deviation after implementing the non-uniformity compensation algorithm may be termed as spatial noise Mathematically it can be expressed as:

$$I_{N,\,spatial} = \left| I_{RO}(T) - I_{RO}(T, \pm\sigma)_{COR} \right| \qquad (3)$$

$I_{RO}(T, \pm\sigma)$ is given by:

$$I_{RO}(T,\pm\sigma)_{COR} = I_{RO}(T_1)[I_{RO}(T,\pm\sigma) - I_{RO}(T_2,\pm\sigma)]\cdot [I_{RO}(T_1,\pm\sigma) - I_{RO}(T_2,\pm\sigma)]^{-1} - I_{RO}(T_2)[I_{RO}(T,\pm\sigma) - I_{RO}(T_1,\pm\sigma)]\cdot [I_{RO}(T_1,\pm\sigma) - I_{RO}(T_2,\pm\sigma)]^{-1} \quad (4)$$

In the above equation, $I_{RO}(T_1)$ and $I_{RO}(T_2)$ are the mean pixel responses at the calibration temperatures T_1 ($= T + dT$) and T_2 ($= T - dT$). These responses can be estimated from the corresponding calculated detector current I_D using the following relation:

$$I_{RO}(T) = I_D(T) - \frac{(n/m)\,kT_f}{(1+A)qR_{DS}} \quad (5)$$

where T_f is the focal plane temperature, A is the gain of the buffer amplifier and (n/m) is the ideality factor of the input MOSFET channel whose numerical value has been taken as 2 in the present work. R_{DS} is the operating point dynamic impedance of the photodiode, which represents the resultant of parallel combination of ideal diode impedance R_D, and contribution of shunt resistance R_S due to surface leakage currents. In Eqn (4) $I_{RO}(T_1, \pm\sigma)$ and $I_{RO}(T_2, \pm\sigma)$ are the uncorrected pixel responses corresponding to the $\pm 1\sigma$ points of the response distribution at T_1 and T_2. These responses can be calculated from the estimated corresponding $I_{RO}(T)$ by applying the following relation:

$$I_{RO}(T, \pm\sigma) = I_{RO}(T) \pm \Delta I_{RO}(T) \quad (6)$$

where $\Delta I_{RO}(T)$ is the rms deviation in the read-out current from its mean value at a given target/ calibration temperature T, arising due to the combined effect of a variety of independent sources responsible for the response non-uniformity in the

$$+\{\Delta I_{RO}(T)\}_{V_T}^2 + \{\Delta I_{RO}(T)\}_{\varepsilon}^2]^{1/2} \quad (7)$$

In Eqn (7), $\Delta(I_{RO})_x$ represents the contribution of compositional variations (Δx) in basic $Hg_{1-x}Cd_xTe$ material used in the fabrication of IR detector array to the read-out current at the output of FPA. It is this part of the response variations which can be reduced using an optical filter. The variations in the output current on account of Δx are the sum of two components, one arising due to the IR detector current variations on account of quantum efficiency and cut-off wavelength variations and the other arising due to injection efficiency variations on account of accompanying changes in diode impedances and operating point of the pixels. The resultant variation is given by[11]:

$$\frac{\Delta I_{RO}}{\Delta x} = \eta\left[1 + \frac{1-\eta}{2-\eta}\left(1 + \frac{q}{kT_f}\frac{R_s R_{DS}}{1+g_{me}R_s}\frac{I_D}{R_D}\right)\right]\left(\frac{\Delta I_D}{\Delta x}\right) + \frac{R_{DS}I_D}{R_O R_D}\frac{\eta(1-\eta)}{2-\eta}\frac{\Delta R_O}{\Delta x} \quad (8)$$

It can be seen from the set of following equations that $\Delta I_{RO}/\Delta x$ can be minimised by minimising $\Delta I_D/\Delta x$. The latter[11] is given by:

$$\frac{\Delta I_D}{\Delta x} = \frac{-\frac{\Delta I_B}{\Delta x} - \frac{\Delta I_T}{\Delta x} + \frac{\Delta I_L}{\Delta x}\left[\exp\left(\frac{qV_B}{kT_f}\right) - 1\right]}{1 + \frac{R_s}{R_D(1+g_{me}R_s)}} \quad (9)$$

$$\frac{\Delta I_B}{\Delta x} = qA_d\left[\eta_d\frac{\Delta\phi_B}{\Delta x} + \phi_B\frac{\Delta\eta_d}{\Delta x}\right] \quad (10)$$

$$\frac{\Delta I_T}{\Delta x} = \frac{qA_d\tau_o\tau_a}{4f^2}\left[\eta_d\frac{\Delta\phi_T}{\Delta x} + \phi_T\frac{\Delta\eta_d}{\Delta x}\right] \quad (11)$$

Equations (9) – (11) predict that $\Delta I_D/\Delta x$ can be minimised by minimising the incident photon flux

contribution of processing-induced variations $[(\Delta I_{RO})_{PROCESS}]$ introduced during processing of the array remains uninfluenced by the optical filter and therefore can be obtained from the following expressions:

$$\left(\frac{\Delta I_{RO}}{\Delta R_{DS}}\right)_{PROCESS} = \eta\left(\frac{3-2\eta}{2-\eta}\right)\frac{(V_B - kT_f/q)R_S}{R_{DS}^2[R_S + R_D(1+g_{me}R_s)]} + \eta\left(\frac{1-\eta}{2-\eta}\right)\frac{I_D}{R_{DS}} \quad (12)$$

where $\Delta R_{DS} = \pm R_{DS}$, if $R_S = R_D$ or $R_S << R_D$ and $\Delta R_{DS} = \pm(R_{DS}-R_D)$, when $R_S >> R_D$. Similarly, the contributions of threshold voltage variations $[(\Delta I_{RO})V_T]$ in the input MOSFET channel and pixel-to-pixel transfer efficiency variations $[(\Delta I_{RO})_\varepsilon]$ in case of CCD-based read-out multiplexers remain independent of optical filter and can be calculated from the following expressions:

$$\left(\frac{\Delta I_{RO}}{\Delta V_T}\right) = \eta\left[1+\frac{1-\eta}{2-\eta}\left(1-\frac{qI_D}{kT_f}\frac{R_{DS}^2 R_S}{R_D(R_S-R_{DS})}\right)\right]\frac{(R_S-R_{DS})}{R_S R_{DS}} \quad (13)$$

$$(\Delta I_{RO})_\varepsilon = n_i \varepsilon^{n_i-1}\eta I_D \Delta\varepsilon \quad (14)$$

3.2 Spatial NETD

Spatial noise-limited NETD of a FPA can be defined as the equivalent change in target temperature T, which produces a unity signal-to-spatial-noise ratio in the FPA, i.e.

$$NETD_{spatial} = \frac{\Delta T}{I_s / I_{N,spatial}} \quad (15)$$

$$= \eta\left[\frac{R_D(1+g_{me}R_S)}{R_D(1+g_{me}R_S)}\right] \quad (16)$$

Minus sign in the above equation indicates the minority carrier contribution to I_S in the photovoltaic IR detectors. The change in the target-induced current (ΔI_T) in the IR detector and the effective injection efficiency (η_{eff}) in a direct injection[10,12] read-out hybrid FPA are respectively given by the following expressions:

$$\Delta I_T = \frac{\eta_d q A_d \tau_o \tau_a}{4f^2}[\phi_{T+\Delta T} - \phi_T] \quad (17)$$

$$\eta_{eff} = \eta\left[1-\frac{1-\eta}{2-\eta}\left(\frac{1}{I_D}+\frac{qR_{DS}R_S}{kT_f R_D(1+g_{me}R_S)}\right)I_D\right] \quad (18)$$

3.3 Temporal NETD

Temporal NETD is essentially the temporal noise-limited NETD of a hybrid pixel of mean response in the FPA and can be estimated by definition from the following relation:

$$NETD_{temporal} = \frac{\Delta T}{I_S / I_{N,temporal}} \quad (19)$$

The temporal noise of the pixel to be substituted[13] in the Eqn (19) is given by[13]:

$$\frac{I_{N,temporal}}{(\Delta f)^{1/2}} = [\eta_{eff}^2 I_{n,det}^2 + (1-\eta_{eff})^2 I_{n,input}^2]^{1/2} \quad (20)$$

where $I_{n,det}$ and $I_{n,input}$ are respectively the noise currents originating in the photodiode and the input structure of the read-out. The bandwidth Δf is approximately related to the T_i by the following relation:

$$\Delta f = \frac{1}{2T_i} \quad (21)$$

temporal and spatial [illegible]

LWIR *HgCdTe* FPAs are presented. The input parameters used in these calculations are summarised in Table 1. As regards the filter characteristics, it is assumed that (i) the filter has a sharp cut-off and that all the incident radiation of wavelength less than its cut-off wavelength is transmitted by the filter without attenuation, and (ii) self-emission from the filter is negligible. The results reported correspond to a mean target temperature of 300K with the calibration temperatures set at 290K and 310K.

The calculated dependence of the spatial noise on the cut-off wavelength of the filter is shown in Figs 2 and 3 for MWIR and LWIR FPAs, respectively. Note that there are two curves marked 1 and 2 representing the two values of the spatial noise plotted for each cut-off wavelength of the filter. Of these, the higher curve marked 1 than the mean response. The difference in the residual spatial noise in the two cases arise because of the pixel-to-pixel variations in response to nonlinearity. The present calculations have been carried out allowing the T_i to vary for compensating the loss of signal on account of smaller cut-off wavelength of the filter than the diode. The charge storage capacity in the read-out array was treated as constant at 2×10^7 e^- for both MWIR and LWIR arrays. The curve marked 4 are the plot of T_i with the change in cut-off wavelength of the filters in the respective arrays. The corresponding temporal noise of the pixels of mean response in each case is shown by the curve marked 3. The improvement in the temporal noise with the reduction in filter cut-off wavelength is due to corresponding increase in T_i. It may be noted from Eqn (20) that the temporal noise is dependent on the bandwidth Δf.

Table 1. Input parameters

Parameter	Symbol	MWIR	LWIR
Mean composition of $Hg_{1-x}Cd_xTe$	x	0.3	0.221
Composition variation	Δx	± 0.001	± 0.001
Detector active area (μm^2)	A_d	50 × 50	50 × 50
Focal plane temperature (K)	T_f	77	77
Spectral window (filter cut-off in μm)		3	8
F-number	f	3	3
Cold shield efficiency (%)		100	100
Emissivity of target & background	$\varepsilon_{T/B}$	1	1
Background temperature (K)	T_B	300	300
Scene/target temperature (K)	T_T	300	300
Transmission coefficient of optics and atmosphere	$\tau_o\tau_a$	1	1
Operating bias	V_B	0	0
Threshold voltage variations in input MOSFET (mV)	ΔV_T	± 5	± 5
Gain of BDI interface	A	–	50
Resistance area product* (Ω cm^2)	R_0A	1×10^9	25

* In this range of R_0A product with the mentioned BDI gain, the reported results are independent of the shunt resistance R_s.

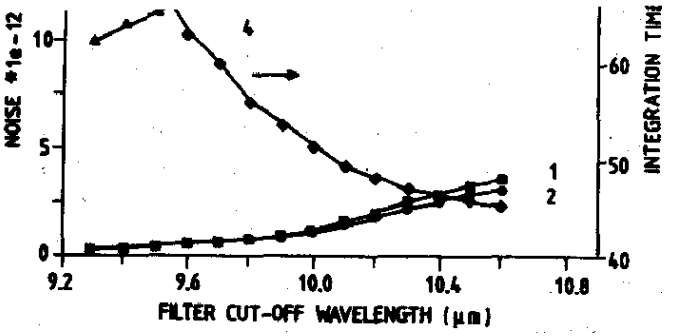

Figure 2. Relative noise contributions *vs* filter cut-off wavelength in a MWIR FPA with average detector cut-off wavelength as 5.1 μm (x = 0.3). The curves marked 1 and 2 correspond to the two values of spatial noise. Whereas the curves marked 3 and 4 represent the temporal noise and integration time. integration time has been treated as variable for the fixed-charge storage capacity of 2×10^7 e⁻.

In staring arrays Δf is inversely proportional to the T_i [Eqn (21)] and hence with increase in T_i Δf decreases, leading to a reduction in the temporal noise.

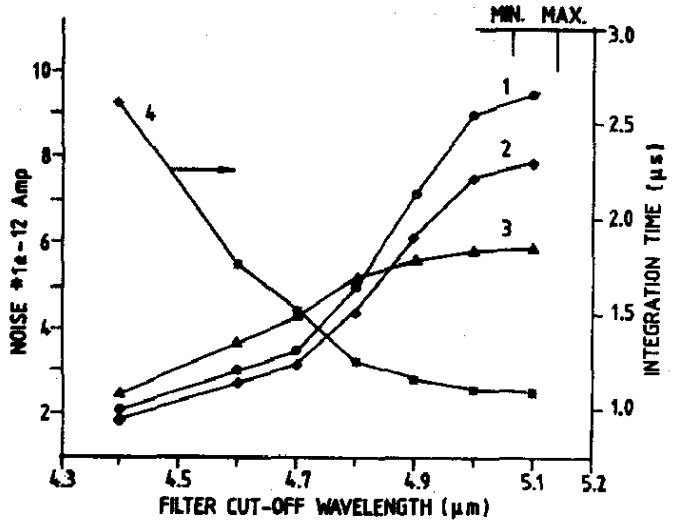

Figure 3. Relative noise contributions *vs* filter cut-off wavelength in a LWIR FPA with average detector cut-off wavelength as 10.6 μm (x = 0.221). The curves marked 1 and 2 correspond to the two values of spatial noise. Whereas the curves marked 3 and 4 represent the temporal noise and integration time, integration time has been treated as variable for the fixed-charge storage capacity of 2×10^7 e⁻.

NETD in the respective figures. Before discussing the effect of filter cut-off wavelength on the performance of FPA, it will be worthwhile to emphasise that the enhancement of T_i to compensate for the loss of signal is unlikely to pose a serious problem in the 2-D staring *HgCdTe* FPAs since T_i (Figs 2 and 3) is less than the practical frame times. For example, in a terrestrial thermal imager that looks for relatively slow moving objects, a frame rate of 30 Hz-60 Hz is considered adequate. In scenarios that have a more demanding temporal response (for example, a missile seeker application), a frame rate of several hundred Hz may become desirable.

It is observed from Figs 2 and 3 that an optical filter has the desired effect of reducing spatial noise in both the spectral windows. Another notable feature is the narrowing the difference in the two values of the residual spatial noise due to the overall improvement in the pixel-to-pixel response non-uniformity with the reduction in the filter cut-off wavelength. It is also seen that the rate of reduction in spatial noise decreases with increasing difference in the filter and the detector cut-off wavelength. Both the features, namely the convergence of the two spatial noise curves coupled with the decreasing rate of reduction in spatial noise point towards an approaching optimum cut-off wavelength of the optical filter.

It is also observed from Figs 4 and 5 that the use of optical filters of smaller cut-off wavelengths than that of photodiodes in a *HgCdTe* FPA will result in considerable improvement of the spatial NETD, whereas the temporal NETD performance will remain unaffected due to proportional reduction in mean temporal noise due to the enhanced T_i and the accompanied loss in signal.

It is also noted from Figs 2 and 4 that due to dominant contribution of spatial noise the performance of a MWIR *HgCdTe* FPA will be limited by the spatial noise rather than by the temporal noise in the absence of an optical filter. However, an optical filter of appropriate cut-off wavelength can result in

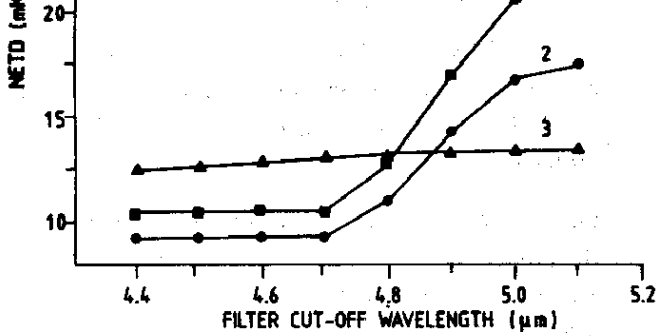

Figure 4. Comparison of spatial (curves 1 and 2) and temporal (curve 3) NETDs as a function of filter cut-off wavelength in a MWIR *HgCdTe* FPA.

considerable improvement in the performance of the MWIR FPA by bringing down the spatial noise to the level of temporal noise contribution.

It is seen from Fig. 5 that the NETD performance of LWIR *HgCdTe* FPA will be limited by the temporal noise and that the spatial noise even without an optical filter matter a little if the charge handling capacity of the read-out multiplexer was 2×10^7 e^-. Obviously in this case, optical filter can

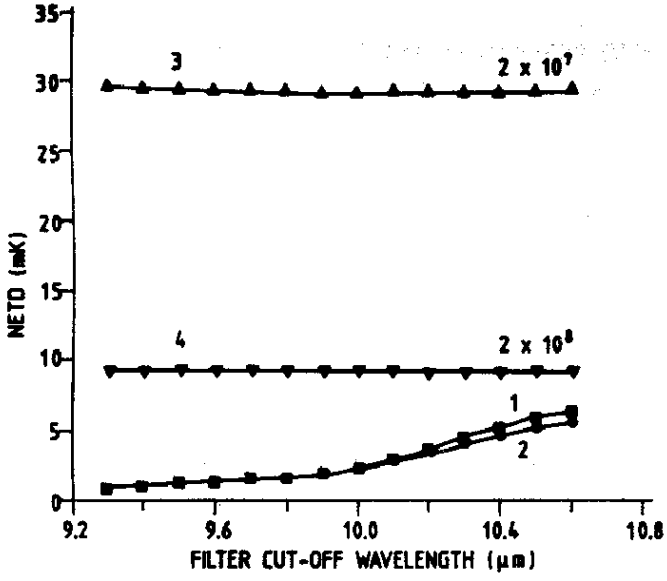

Figure 5. Comparison of spatial (curves 1 and 2) and temporal (curves 3 and 4) NETDs as a function of filter cut-off wavelength in a LWIR *HgCdTe* FPA. The curves 3 and 4 were obtained for two different charge storage capacities marked on the respective curves.

reducing the spatial noise.

5. CONCLUSIONS

It is concluded that the use of an optical filter, whose cut-off wavelength is much less than the detector cut-off wavelength, can lead to considerable reduction in the spatial noise of both MWIR and LWIR *HgCdTe* FPAs. These filters can be thus used either to reduce the spatial noise or trade-off the requirement of composition uniformity of *HgCdTe* substrate, depending upon the relative magnitude of temporal and spatial noise components.

ACKNOWLEDGEMENT

Authors are thankful to Director, Solidstate Physics Laboratory (SPL), Delhi, for the constant encouragement and permission to publish this work.

REFERENCES

1. Carrison, C.L. & Foss, N.A. Fixed-pattern noise compensation techniques for staring IR focal planes. *Optical Engineering*, 1980, **19**, 753-57.

2. Milton, A.F.; Barone F.R. & Kruer, M.R. Influence of non-uniformity on infrared focal plane array performance. *Optical Engineering*, 1985, **24**, 855-62.

3. Boreman, G.D. & Constanzo, C. Compensation for gain non-uniformity and nonlinearity in *HgCdTe* infrared charge couple device focal planes. *Optical Engineering*, 1987, **26**, 981-84.

4. Poropat, G.V. Nonlinear compensation for responsivity non-uniformity in cadmium mercury telluride focal plane detectors for use in the 8 to 12 μm spectral region. *Optical Engineering*, 1989, **28**, 887-96.

6. Perry, D.L. & Dennak, E.L. Linear theory of nonuniformity correction in infrared staring sensors. *Optical Engineering*, 1993, **32**, 1854-859.

7. Schulz, M. & Caldwell, L. Non-uniformity correction and correctability of infrared focal plane arrays *Infrared Phy. Technol.*, 1995, **36**, 763-777.

8. Hansen, G.L.; Schmit, J.L. & Casselman, T.N. Energy gap versus alloy composition and temperature in Hg_{1-x} Cd_xTe. *J. Appl. Phys.* 1982, **53**, 7099-101.

Optical Engineering, 1992, **31**, 2350.

11. Gopal, Vishnu. Model for response non-uniformity calculations of DI read-out hybrid focal plane array. *Optical Engineering*, 1994, **33**, 809-19.

12. Gopal, Vishnu. Noise equivalent temperature difference performance of an IR detector in a hybrid focal plane array. *Infrared Phy. Technol.*, 1995, **36**, 937-48.

13. Gopal, Vishnu. Achieving BLIP performance in a direct injection read-out hybrid focal plane array. *Proceedings SPIE*, 1994, **2225**, 299-309.